

RESEARCH ARTICLE

Dynamic contrast-enhanced magnetic resonance imaging in denervated skeletal muscle: Experimental study in rabbits

Liang Qi¹, Lei Xu¹, Wen-Tao Wang¹, Yu-Dong Zhang¹, Rui Zhang², Yue-Fen Zou¹, Hai-Bin Shi¹[†]*

1 Department of Radiology, The First Affiliated Hospital of Nanjing Medical University, Nanjing, PR China,

2 Department of Neurosurgery, Nanjing Children's Hospital, Nanjing, PR China

[†] These authors contributed equally to this work.

^{‡a} Current address: Department of Radiology, The First Affiliated Hospital of Nanjing Medical University, Nanjing, PR, China

^{‡b} Current address: Department of Neurosurgery, Nanjing Children's Hospital, Nanjing, PR China

* haibinshi1120@126.com



OPEN ACCESS

Citation: Qi L, Xu L, Wang W-T, Zhang Y-D, Zhang R, Zou Y-F, et al. (2019) Dynamic contrast-enhanced magnetic resonance imaging in denervated skeletal muscle: Experimental study in rabbits. PLoS ONE 14(4): e0215069. <https://doi.org/10.1371/journal.pone.0215069>

Editor: Xi Chen, McLean Hospital, UNITED STATES

Received: November 3, 2018

Accepted: March 26, 2019

Published: April 5, 2019

Copyright: © 2019 Qi et al. This is an open access article distributed under the terms of the [Creative Commons Attribution License](https://creativecommons.org/licenses/by/4.0/), which permits unrestricted use, distribution, and reproduction in any medium, provided the original author and source are credited.

Data Availability Statement: All relevant data are within the manuscript and its Supporting Information files.

Funding: This study was funded by the National Natural Science Foundation of China (grant number 81701652), which was received by Liang Qi. The URL is <https://isisn.nsf.gov.cn>. The funders had no role in study design, data collection and analysis, decision to publish, or preparation of the manuscript.

Competing interests: The authors have declared that no competing interests exist.

Abstract

Purpose

To investigate the value of dynamic contrast-enhanced (DCE) magnetic resonance imaging (MRI) for evaluating denervated skeletal muscle in rabbits.

Materials and methods

24 male rabbits were randomly divided into an irreversible neurotmesis group and a control group. In the experimental group, the sciatic nerves of rabbits were transected for irreversible neurotmesis model. A sham operation was performed in the control group. MRI of rabbit lower legs was performed before nerve surgery and 1 day, 3 days, 5 days, 1 week, 2 weeks, 3 weeks, 4 weeks, 6 weeks, 8 weeks, 10 weeks, and 12 weeks after surgery.

Results

Signal intensity changes were seen in the left gastrocnemius muscle on the T2-weighted images. DCE-MRI derived parameters (K^{trans} , K_{ep} , and V_p) were measured in vivo. In the irreversible neurotmesis group, T2-weighted images showed increased signal intensity in the left gastrocnemius muscle. K^{trans} , V_p values changes occur as early as 1 day after denervation, and increased gradually until 4 weeks after surgery. There are significant increases in both K^{trans} and V_p values compared with those in the control group after surgery ($P < 0.05$). K_{ep} values show no significant difference between the irreversible neurotmesis group and the control group.

Conclusion

DCE-MRI hold the promise of an early and sensitive diagnosis of denervated skeletal muscle.

Introduction

Peripheral nerve injury leads to morphologic and metabolic changes in the target denervated skeletal muscles. Electromyography (EMG) is useful for the diagnosis of denervated muscles [1]. However, EMG sometimes presents some difficulties in the detection of denervated skeletal muscle because it is both invasive and dependent on the skill of the examiner, and it is difficult to obtain information that is useful, objective, and reproducible with EMG in the deep muscles or small intramuscular areas.

Conventional magnetic resonance imaging (MRI) has proved to be useful in the diagnosis of denervated skeletal muscle after peripheral nerve injury [2–5]. Denervated skeletal muscle usually show high signal intensity on T2-weighted MR images and normal signal intensity on T1-weighted MR images. Numerous previous articles have corroborated these findings [2, 3, 5–8].

Recently, there have been a few of investigations of functional MR imaging in the evaluation of denervated skeletal muscle [9–11]. Some previous studies found that acute and subacute denervated skeletal muscles showed increased T2, apparent diffusion coefficient (ADC) and decreased fractional anisotropy on T2 mapping, diffusion-weighted imaging (DWI), and diffusion tensor imaging (DTI), respectively [12–18]. Another functional MR imaging, dynamic contrast-enhanced (DCE) T1-weighted MR perfusion imaging, is also available. With the recent improvements in functional MR imaging, tissue perfusion assessment with DCE-MRI is routinely performed in neurology, oncology and cardiology as well as, more recently, in the imaging of ischemic skeletal muscle [19–21]. To our knowledge, few articles have used this technique to assess the denervated skeletal muscle after peripheral nerve injury. Therefore, the purpose of our study was to determine the value of DCE-MRI for evaluating the early state of denervated skeletal muscle in nerve injury models in rabbits.

Materials and methods

Experimental model

This study was carried out in strict accordance with the recommendations in the Guide for the Care and Use of Laboratory Animals of the National Institutes of Health. The protocol was approved by the Committee on the Ethics of Animal Experiments of The First Affiliated Hospital of Nanjing Medical university (Protocol Number: 25783). All surgery was performed under sodium pentobarbital anesthesia, and all efforts were made to minimize suffering. The animals were held in separate cages in a clean environment with proper temperature and humidity. The rabbits were subjected to 12h light /dark cycle and allowed to have food and water ad libitum. Viability and behavior were recorded every day, and body weight was recorded twice weekly. If the rabbits presented with signs of suffering (pain, weakening) or loss of more than 15% of baseline weight, the animals were humanely killed considered. We used a total of 24 male New White rabbits, each of which weighted approximately 3kg. The rabbits was numbered from 1 to 24 according to the body weight, using the random number table, the animals were divided into an irreversible neurotmesis group (group A) and a control group (group B), there were 12 rabbits in each group. The rabbits were anesthetized with 30 mgkg⁻¹ of pentobarbital sodium (Nembutal; Bayer, Leverkusen, Germany) injected into the external ear vein. In the group A, a 3cm incision of the skin was made on the left proximal hind limb at the level of the hip bone. The sciatic nerve was exposed at the sciatic notch, we transected and removed 1cm length of sciatic nerve for a complete irreversible neurotmesis model. In the group B, we performed sham operations (incision and exploration of the sciatic nerve only) at the same time. To avoid infection, 800000 units of penicillin (HenRui Co,

China) were administered via intramuscular injection over the 7 days following operation. Ketoprofen (1.0mg/kg, once daily, (Xinan Pharmaceutical Factory, China) were subcutaneously injected for three days. All surgical procedures were performed by an author who had 10 years of experience with microsurgical procedures.

MRI acquisition technique

MR studies was performed before nerve surgery and was repeated 1 day, 3 days, 5 days, 1week, 2 weeks, 3weeks 4 weeks, 6 weeks, 8 weeks, 10 weeks and 12 weeks after surgery. A venous indwelling needle (24 Gauge) was inserted into a lateral ear vein and secured for intravenous administration of anesthetics and MR contrast agent. All examinations were conducted on a 3 Tesla MR unit (Magnetom Trio Tim; Siemens, Erlangen, Germany). The measurements were performed with the rabbits under anesthesia and in a prone position with both hind limbs positioned in a dedicated eight-channel knee coil (Invivo, Gainesville, FL, USA). The MRI protocol included the following sequences: (1) Axial T1-weighted by turbo spin-echo (TSE) sequence images were obtained by using the following parameters: repetition time (TR), 824ms; echo time (TE), 22ms; matrix size, 320 × 320; field of view (FOV), 120 × 120mm; slice thickness, 3mm. (2) Axial T2-weighted images by TSE with fat suppression was obtained with the following parameters: TR, 4000; TE, 52; matrix size 320 × 320; FOV, 120 × 120mm; slice thickness, 3mm; (3) In the term of DCE imaging, for the baseline T1 mapping, unenhanced T1-weighted volume interpolated gradient echo (VIBE) images were acquired at each of the 3 flip angles using the following parameters: TR, 4.6ms; TE, 1.6ms; flip angle (FA), 2°, 8°, and 15°; FOV, 120× 120mm; matrix, 192 × 192; slice thickness, 3 mm. Then, DCE MR imaging using a radial three-dimensional VIBE with k-space-weighted image contrast reconstruction was performed. After 3 acquisitions, a bolus injection of 0.1 mmol/kg Gd-DTPA (gadopentate dimeglumine, Magnevist, Bayer Schering, Berlin, Germany) was injected at a rate of 1 mL/s through the venous indwelling needle. Bolus injection was performed with a MR-compatible power injector (Spectris; Medrad, Pittsburgh, PA) followed by a 2-mL saline flush. The parameters were as follows: TR, 4.6ms; TE, 1.6ms; FA, 11°; FOV, 120× 120mm; matrix, 192 × 192; slice thickness, 3mm; time resolution per measurement, 6 seconds; total scan duration, 10min.

Image analysis

We subjectively classified signal intensity changes in the denervated gastrocnemius muscle into the following four grades: grade 0 (iso-signal intensity compared with that in the control group); grade 1 (slightly hyperintense); grade 2 (intermediate to high signal intensity); grade 3 (high signal intensity). Two authors (more than 10 years of experience with musculoskeletal MR imaging) evaluated the images in consensus.

The DCE-MRI data was post-processed by in-house software (OmniKinetics Version 2.0, GE Healthcare, China). The current tracer-kinetic modeling for quantitation of DCE images are based on a modified tofts model [22]. The model describes the tissue as a combination of a vascular compartment and an extracellular extravascular compartment, the following concentration-time equation was used:

$$C(t) = K^{trans} \int_0^t C_p(\tau) e^{k_{ep}(t-\tau)} d\tau + v_p C_p(t) \quad (1)$$

Where K^{trans} is the volume transfer constant between blood plasma and the extracellular extravascular space (EES); K_{ep} is the rate constant between the EES and blood plasma; V_p is blood plasma volume fraction; $C_p(\tau)$ is the concentration-time curve in the arterial blood plasma. For quantitation of DCE images, the contrast concentration was semi-quantitated by using relative signal intensity enhancement ratio. For the purpose of the vascular input

function (VIF), a region of interest (ROI) was placed in the popliteal artery, the mean size of ROIs was 4 mm^2 (range, 3–5 mm^2). Then the pixel-by-pixel plots of K^{trans} , K_{ep} and V_p maps were automatically constructed by a Levenberg-Marquardt nonlinear least squares algorithm. ROIs were manually drawn on all imaging sections to acquire a volume of interest (VOI) of gastrocnemius muscle, and an effort was made to exclude fatty septa and vessels. Then, the mean K^{trans} , K_{ep} , and V_p values derived from Color-coded parametric maps were obtained. The mean VOIs of the gastrocnemius muscle were $4.54 \pm 2.18 \text{ cm}^3$. The above DCE parameters were measured by two independent observers (more than 10 years of experience with musculoskeletal MR imaging, respectively) who were blinded to the group allocations. The results acquired from two observers were averaged and used for analysis.

EMG study

A Cadwell Sierra (Neuropack Four Mini; Nihon Kohden, Tokyo, Japan) computer-based EMG unit was used for electrodiagnostic studies, two rabbits randomly selected from each group were again anesthetized, and a conventional concentric needle electrode was placed in the left gastrocnemius muscle. We looked for abnormal spontaneous activity (positive sharp waves or fibrillation). The measurements were performed before nerve surgery and were repeated at 1 day, 3 days, 5 days, 1 week, 2 weeks, 3 weeks, 4 weeks, 6 weeks, 8 weeks, 10 weeks and 12 weeks after surgery by an author who had 10 years of experience with EMG.

Statistical analysis

All statistical analyses were performed using SPSS 17.0 (SPSS, Inc., Chicago, IL, USA). Continuous variables were expressed as mean \pm standard deviation (SD). Interobserver reliability of the measurements was assessed by using the intraclass correlation coefficient (ICC). The ICC was interpreted as follows: poor agreement (ICC = 0); minor agreement (ICC = 0–0.2); fair agreement (ICC = 0.21–0.40); moderate agreement (ICC = 0.41–0.60); good agreement (ICC = 0.61–0.8), perfect agreement (ICC = 0.81–1.00). K^{trans} , K_{ep} , and V_p values of specific acquisition points within groups were compared by using repeated-measures analysis of variance. Comparisons between the two groups at each acquisition point were performed by using one-way analysis of variance (ANOVA) test, statistical significances was considered when P value of less than 0.05.

Results

Changes in signal intensity

In the irreversible neurotmesis group (Group A), T2-weighted images with fat suppression showed slightly hyperintense in the target gastrocnemius muscle beginning 5 days after surgery, at 3 weeks, high signal intensity were observed. For all rabbits in this group, signal intensity remained high until 12-week follow up (Table 1).

Quantitative DCE MR imaging parameters

Kappa values (κ) of 0.823, 0.852, and 0.792 for K^{trans} , K_{ep} , and V_p , respectively, show good interobserver agreement.

In the irreversible neurotmesis group (group A), K^{trans} , V_p values increased gradually until 4 weeks after surgery and remained high (mean, approximately $15.391 \pm 2.829 \times 10^{-2} \text{ min}^{-1}$ and $3.893 \pm 0.890 \times 10^{-1}$, respectively,) throughout the remainder of the study period (Tables 2 and 3, Figs 1, 2 and 3). In this group, we observed significant increases in both K^{trans} and V_p values compared with those in the control group during the period from 1 day after surgery to

Table 1. Classification of signal intensity changes for each injury group.

Follow-up interval	Group A (n = 12)				Group B (n = 12)			
	Grade 0	Grade 1	Grade 2	Grade 3	Grade 0	Grade 1	Grade 2	Grade 3
Before	12				12			
1 d	12				12			
3 d	12				12			
5 d	2	10			12			
1 W		12			12			
2 W		3	9		12			
3 W			1	11	12			
4 W				12	12			
6 W				12	12			
8 W				12	12			
10 W				12	12			
12 W				12	12			

W = week.

<https://doi.org/10.1371/journal.pone.0215069.t001>

12 weeks after surgery (Tables 2 and 3, Figs 1, 2 and 3). K^{trans} values increased significantly during the periods from pre-operation to 1 day after surgery ($P = 0.029$), from 1 day after surgery to 3 days after surgery ($P < 0.001$), from 3 days after surgery to 5 days after surgery ($P < 0.001$), from 5 days after surgery to 1 week after surgery ($P < 0.001$), from 1 week after surgery to 2 weeks after surgery ($P < 0.001$), from 2 weeks after surgery to 4 weeks after surgery ($P < 0.001$). V_p values increased significantly during the periods from pre-operation to 1 day after surgery ($P < 0.001$), from 1 day after surgery to 3 days after surgery ($P = 0.001$), from 3 days after surgery to 1 week after surgery ($P < 0.001$), from 1 week after surgery to 2 weeks after surgery ($P = 0.007$). From 2 weeks after surgery to 4 weeks after surgery ($P = 0.001$). However, K_{ep} values show no significant difference between the irreversible neurotmesis group and the control group.

Table 2. Mean K^{trans} values for each injury group.

Follow-up interval	Group A ($\times 10^{-2} \text{ min}^{-1}$)	Group B ($\times 10^{-2} \text{ min}^{-1}$)	P-Value
Before	0.904 ± 0.425	0.812 ± 0.424	0.600
1 d	1.444 ± 0.675	0.844 ± 0.294	0.010*
3 d	2.743 ± 0.806	0.921 ± 0.397	< 0.001*
5 d	4.540 ± 0.969	0.868 ± 0.428	< 0.001*
1 W	7.247 ± 0.999	0.874 ± 0.338	< 0.001*
2 W	10.859 ± 1.441	0.876 ± 0.468	< 0.001*
3 W	14.308 ± 3.722	0.881 ± 0.417	< 0.001*
4 W	15.391 ± 2.829	0.962 ± 0.282	< 0.001*
6 W	16.315 ± 3.672	0.975 ± 0.552	< 0.001*
8 W	17.858 ± 5.304	0.944 ± 0.479	< 0.001*
10 W	15.689 ± 5.086	0.929 ± 0.588	< 0.001*
12 W	16.628 ± 5.339	0.900 ± 0.426	< 0.001*

W = week. P-value represents the comparison results between group A and B by the one-way analysis of variance analysis.

*P values indicate statistical significance.

<https://doi.org/10.1371/journal.pone.0215069.t002>

Table 3. Mean V_p values for each injury group.

Follow-up interval	Group A ($\times 10^{-1}$ ml/ml)	Group B ($\times 10^{-1}$ ml/ml)	P-Value
Before	0.218 \pm 0.037	0.210 \pm 0.031	0.594
1 d	0.834 \pm 0.217	0.217 \pm 0.085	< 0.001*
3 d	1.287 \pm 0.299	0.182 \pm 0.055	< 0.001*
5 d	1.646 \pm 0.470	0.217 \pm 0.087	< 0.001*
1 W	2.097 \pm 0.435	0.187 \pm 0.064	< 0.001*
2 W	2.717 \pm 0.546	0.201 \pm 0.113	< 0.001*
3 W	3.164 \pm 1.221	0.225 \pm 0.100	< 0.001*
4 W	3.893 \pm 0.890	0.188 \pm 0.082	< 0.001*
6 W	4.179 \pm 0.967	0.194 \pm 0.050	< 0.001*
8 W	4.253 \pm 0.974	0.195 \pm 0.056	< 0.001*
10 W	4.218 \pm 1.120	0.236 \pm 0.057	< 0.001*
12 W	4.197 \pm 1.472	0.216 \pm 0.088	< 0.001*

W = week. P-value represents the comparison results between group A and B by the one-way analysis of variance analysis.

*P values indicate statistical significance.

<https://doi.org/10.1371/journal.pone.0215069.t003>

EMG study

In the irreversible axonotmesis group (group A), spontaneous activity was observed at 2-week follow-up; in the control group (group B). EMG was completely normal throughout the study period.

Discussion

As in other studies, we demonstrate here that denervated skeletal muscle in the acute and sub-acute phase characteristically show high signal intensity on T2-weighted MR images [5, 6, 9]. However, to our knowledge, few studies available to date have used DCE MR imaging to evaluate denervated skeletal muscle. In this study, we evaluated the utility of DCE MR imaging for assessing denervated skeletal muscles in rabbits. Among the three different DCE MR imaging-derived parameters (K^{trans} , K_{ep} , and V_p values) used in this study, we found that compared to

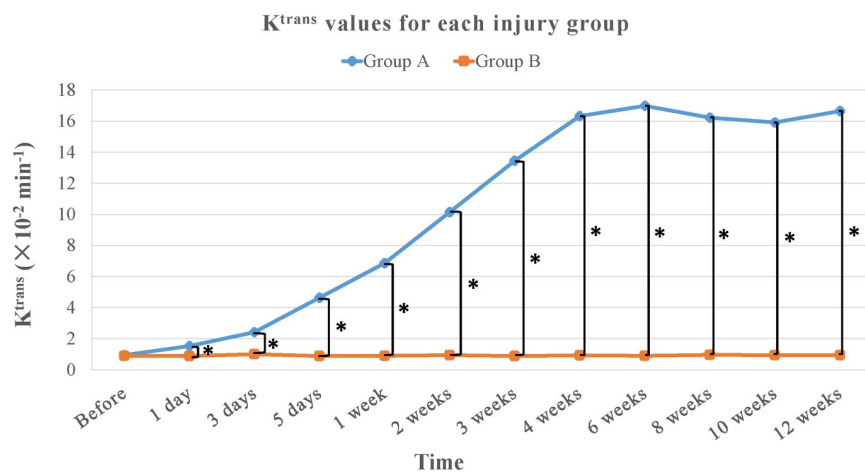


Fig 1. Graph shows the time course of K^{trans} values for each injury group. There were significant differences between irreversible neurotmesis group (group A, blue line) and control group (group B, orange line) after surgery ($P < 0.05$). * = $P < 0.05$.

<https://doi.org/10.1371/journal.pone.0215069.g001>

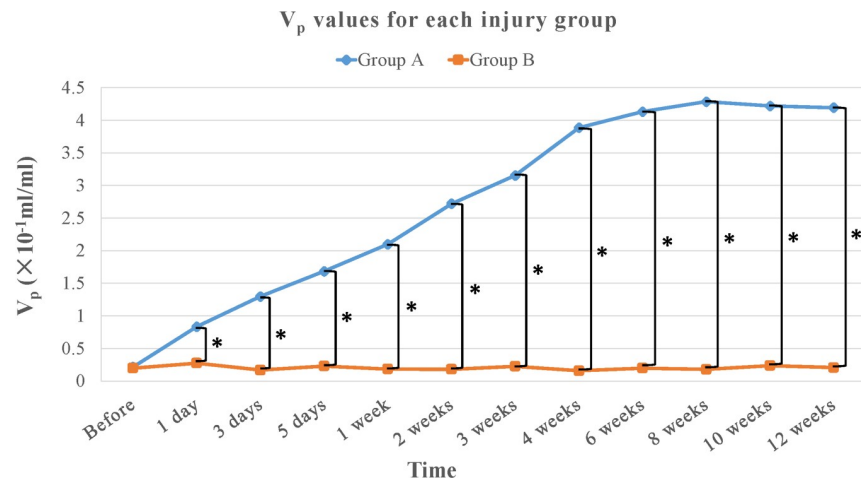


Fig 2. Graph shows the time course of V_p values for each injury group. There were significant differences between irreversible neurotmesis group (group A, blue line) and control group (group B, orange line) after surgery ($P < 0.05$). $*$ = $P < 0.05$.

<https://doi.org/10.1371/journal.pone.0215069.g002>

the uninjured nerves group (group A) showed a significant increase in K^{trans} and V_p values of denervated skeletal muscle after surgery.

For DCE MR imaging parameters, we found K^{trans} and V_p values increased significantly in the irreversible axonotmesis groups compared those in the control group during the stage of denervation. MR contrast agent Gd-DTPA does not enter the intracellular compartment and passes freely through the endothelial barrier with a rapid equilibrium between the interstitial and intravascular space [23]. Therefore, the increased K^{trans} and V_p values could be caused by a dilatation of the vascular bed, an enlargement of the extracellular space, or both. A previous study by Wessig et al found a significant increase of muscle capillaries at 2 days after denervation, and peak capillary enlargement was reached at 4 weeks follow up [24]. Another study by Eisenberg et al using radiolabeled microspheres in rats found a ten-fold increase in blood flow in denervated skeletal muscle. Several other experimental studies also have suggested that injury of sympathetic vasoconstriction leads to increased blood volume in denervated skeletal muscle [11, 25–27]. In the study by Yamabe et al and Holl et al, they demonstrated that extracellular fluid space significantly increased in the denervated skeletal muscle. Denervation causes increases in proteolysis [28], and the permeability muscle cell membrane [29], and decrease in protein synthesis and glycolysis [30]. Also, loss of neurotrophic factor [31], disuse atrophy caused by immobilization, and functional disability of Na,K-ATPase may occur [32]. All of these changes could increase the extracellular water volume. In the present study, we found increase of K^{trans} and V_p values in denervated skeletal muscle as early as 1 day after surgery, i.e., about 2 weeks before the appearance of EMG abnormalities. Compared with signal intensity changes, the K^{trans} and V_p values obtained from DCE MR imaging further narrowed this diagnostic gap.

K_{ep} values represents the flux rate constant between the EES and blood plasma, in the present study, there was no significant differences in K_{ep} values between the irreversible axonotmesis group and the control group. In our opinion, it may be due to contrast enhanced pattern. In our study, we found that both the denervated skeletal muscle and normal skeletal muscle in the rabbits showed persistent pattern (type-I) time-intensity curve (TIC). During the scan time, the contrast in the skeletal muscle constantly full-filled into the EES. Considered that K_{ep} is the flux rate constant from EES to blood plasma, it was not surprising to find that there was no significant difference in K_{ep} values between these two groups.

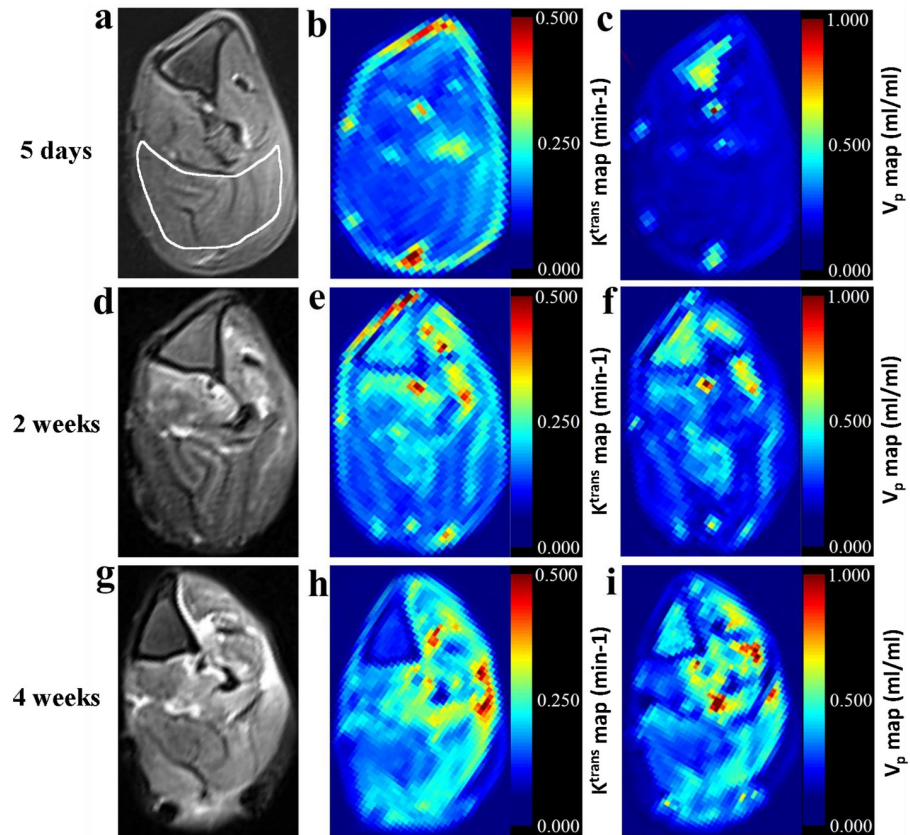


Fig 3. Axial fat-suppressed T2-weighted MR images of the left gastrocnemius muscle (outlined muscle in image) obtained with rabbits in the prone position. (a): At 5 days after surgery, image shows grade 1 signal intensity (ie, signal intensity was isointense or slightly hyperintense compared with that in the control group). (b, c): Color-coded parametric maps are derived from DCE MR imaging. Corresponding K^{trans} and V_p values are $4.513 \times 10^{-2} \text{ min}^{-1}$, 0.152 ml/ml , respectively. (d): At 2 weeks after surgery, image shows grade 2 signal intensity (ie, intermediate to high signal intensity compared with that in the control group). (e, f): Color-coded parametric maps are derived from DCE-MR imaging. Corresponding K^{trans} and V_p values are $11.681 \times 10^{-2} \text{ min}^{-1}$, 0.272 ml/ml , respectively. (g): At 4 weeks after surgery, image shows grade 3 signal intensity (ie, high signal intensity compared with that in the control group). (h, i): Color-coded parametric maps are derived from DCE MR imaging. Corresponding K^{trans} and V_p values are $16.203 \times 10^{-2} \text{ min}^{-1}$, 0.422 ml/ml , respectively.

<https://doi.org/10.1371/journal.pone.0215069.g003>

MRI changes in denervated skeletal muscles were first described by Polak et al in 1988 [7], Fifteen days after transection of the sciatic nerves in rats, prolongation of T2 TR was observed in the denervated skeletal muscles of the lower legs. Thereafter, some other studies also demonstrated that the denervated skeletal muscles presented with high signal intensity on T2-weighted MR images. This phenomenon of high signal intensity on T2-weighted image in denervated skeletal muscles might correlate with an increase in extracellular fluid [6, 7, 9].

In the present study, denervated skeletal muscles showed increased signal intensity that started 5 days after surgery, and presented continuously high signal intensity from 3 weeks after surgery. The time course of signal intensity changes seen on T2-weighted MR images of denervated skeletal muscle in our study was inconsistent with those in previous reports. The study by Holl et al demonstrated that increased signal intensity in denervated skeletal muscle occurred as early as 1 day after sciatic nerve axotomy [9], whereas in another study by Küllmer et al, increased signal intensity on T2-weighted images in denervated skeletal muscle has been shown to occur as early as 3 weeks after suprascapular nerve transection [33]. This discrepant

results might be due to different nerve injury pattern [8], denervation develops earlier when the nerve was cut near the muscle. Long peripheral nerve stump allows a longer release of neurotrophic and protective factors than short stump [7].

In our study, the EMG findings after experimental denervation were consistent with those in the literature [6, 8], about 2–3 weeks after denervation, the first changes (spontaneous activity) were found. When compared with EMG findings, the observed MR signal changes were an early phenomenon occurred about one week before the earliest EMG abnormalities after experimental denervation in rabbits.

Our study had some limitations. First, the results of kinetic parameters may vary when using different post-processing model, and it may also be influenced by following factors: MR scanning parameters, vascular input function, methods for T1 measurement, and injection rate of contrast agent. However, this is common issue which was reported by many previous researches, and we will not address it in this study. Second, in our study, we used a 6-second temporal resolution, relatively lower than those of established articles [34, 35]. The low temporal resolution may result in an underestimate of the VIF, thus leading to overestimate V_p and K^{trans} values of skeletal muscle. This was a technical limitation because our current MR sequences did not support faster scanning for so large imaging coverage. After all, the quantitative results here reflect significant differences between injured and control groups, which demonstrate that DCE is a reliable tool to determine early and time-course hemodynamic changes in denervated skeletal muscles in a rabbit model. Third, the present study focused only on complete nerve transection. Less severe nerve damage and regeneration was not considered in this study. However, an article by Yamable et al. demonstrated that T2 ratios depended on the degree of nerve injury, the more severe the nerve damage, the higher signal intensity on T2-weighted images [8]. Forth, we consider the results to be consistent with changes at MR imaging in human muscle. Further clinical study will be needed in human subject.

Conclusion

In summary, K^{trans} and V_p values obtained from DCE MR imaging parameters changes occur as early as 1 day after denervation. Increased K^{trans} and V_p values is an early phenomenon markedly preceding not only EMG abnormalities but also signal intensity changes after nerve transection. DCE MR imaging hold the promise of an early and sensitive diagnosis of denervated skeletal muscle.

Supporting information

S1 Tables. Data of the dynamic contrast-enhanced magnetic resonance imaging in denervated skeletal muscle: experimental study in rabbits.

(PDF)

S1 Appendix. The ARRIVE guidelines checklist (Animal research: Reporting in vivo experiment).

(PDF)

Author Contributions

Conceptualization: Hai-Bin Shi.

Data curation: Lei Xu, Rui Zhang.

Formal analysis: Wen-Tao Wang, Yue-Fen Zou.

Funding acquisition: Liang Qi.

Investigation: Liang Qi, Yu-Dong Zhang.

Methodology: Lei Xu, Yu-Dong Zhang, Rui Zhang.

Project administration: Liang Qi, Yue-Fen Zou.

Resources: Liang Qi, Yu-Dong Zhang.

Software: Lei Xu.

Supervision: Hai-Bin Shi.

Visualization: Wen-Tao Wang, Rui Zhang.

Writing – original draft: Liang Qi.

Writing – review & editing: Hai-Bin Shi.

References

1. Thesleff S, Ward MR. Studies on the mechanism of fibrillation potentials in denervated muscle. *The Journal of physiology*. 1975; 244(2):313–23. PMID: [1142121](#); PubMed Central PMCID: PMC1330764.
2. Shabas D, Gerard G, Rossi D. Magnetic resonance imaging examination of denervated muscle. *Computerized radiology: official journal of the Computerized Tomography Society*. 1987; 11(1):9–13. PMID: [3581817](#).
3. Fleckenstein JL, Watumull D, Conner KE, Ezaki M, Greenlee RG Jr., Bryan WW, et al. Denervated human skeletal muscle: MR imaging evaluation. *Radiology*. 1993; 187(1):213–8. <https://doi.org/10.1148/radiology.187.1.8451416> PMID: [8451416](#).
4. Uetani M, Hayashi K, Matsunaga N, Imamura K, Ito N. Denervated skeletal muscle: MR imaging. *Work in progress. Radiology*. 1993; 189(2):511–5. <https://doi.org/10.1148/radiology.189.2.8210383> PMID: [8210383](#).
5. West GA, Haynor DR, Goodkin R, Tsuruda JS, Bronstein AD, Kraft G, et al. Magnetic resonance imaging signal changes in denervated muscles after peripheral nerve injury. *Neurosurgery*. 1994; 35(6):1077–85; discussion 85–6. PMID: [7885552](#).
6. Kikuchi Y, Nakamura T, Takayama S, Horiuchi Y, Toyama Y. MR imaging in the diagnosis of denervated and reinnervated skeletal muscles: experimental study in rats. *Radiology*. 2003; 229(3):861–7. <https://doi.org/10.1148/radiol.2293020904> PMID: [14576445](#).
7. Polak JF, Jolesz FA, Adams DF. Magnetic resonance imaging of skeletal muscle. Prolongation of T1 and T2 subsequent to denervation. *Investigative radiology*. 1988; 23(5):365–9. PMID: [3384617](#).
8. Yamabe E, Nakamura T, Oshio K, Kikuchi Y, Ikegami H, Toyama Y. Peripheral nerve injury: diagnosis with MR imaging of denervated skeletal muscle—experimental study in rats. *Radiology*. 2008; 247(2):409–17. <https://doi.org/10.1148/radiol.2472070403> PMID: [18372449](#).
9. Holl N, Echaniz-Laguna A, Bierry G, Mohr M, Loeffler JP, Moser T, et al. Diffusion-weighted MRI of denervated muscle: a clinical and experimental study. *Skeletal radiology*. 2008; 37(12):1111–7. <https://doi.org/10.1007/s00256-008-0552-2> PMID: [18682930](#).
10. Ha DH, Choi S, Kang EJ, Park HT. Diffusion tensor imaging and T2 mapping in early denervated skeletal muscle in rats. *Journal of magnetic resonance imaging: JMRI*. 2015; 42(3):617–23. <https://doi.org/10.1002/jmri.24818> PMID: [25504841](#).
11. Goyault G, Bierry G, Holl N, Lhermitte B, Dietemann JL, Beregi JP, et al. Diffusion-weighted MRI, dynamic susceptibility contrast MRI and ultrasound perfusion quantification of denervated muscle in rabbits. *Skeletal radiology*. 2012; 41(1):33–40. <https://doi.org/10.1007/s00256-011-1108-4> PMID: [21308468](#).
12. Kim HK, Laor T, Horn PS, Racadio JM, Wong B, Dardzinski BJ. T2 mapping in Duchenne muscular dystrophy: distribution of disease activity and correlation with clinical assessments. *Radiology*. 2010; 255(3):899–908. <https://doi.org/10.1148/radiol.10091547> PMID: [20501727](#).
13. Maillard SM, Jones R, Owens C, Pilkington C, Woo P, Wedderburn LR, et al. Quantitative assessment of MRI T2 relaxation time of thigh muscles in juvenile dermatomyositis. *Rheumatology*. 2004; 43(5):603–8. <https://doi.org/10.1093/rheumatology/keh130> PMID: [14983103](#).
14. Kim HK, Laor T, Horn PS, Wong B. Quantitative assessment of the T2 relaxation time of the gluteus muscles in children with Duchenne muscular dystrophy: a comparative study before and after steroid

- treatment. *Korean journal of radiology*. 2010; 11(3):304–11. <https://doi.org/10.3348/kjr.2010.11.3.304> PMID: 20461184; PubMed Central PMCID: PMC2864857.
15. Ponrartana S, Ramos-Platt L, Wren TA, Hu HH, Perkins TG, Chia JM, et al. Effectiveness of diffusion tensor imaging in assessing disease severity in Duchenne muscular dystrophy: preliminary study. *Pediatric radiology*. 2015; 45(4):582–9. <https://doi.org/10.1007/s00247-014-3187-6> PMID: 25246097.
 16. Zaraiskaya T, Kumbhare D, Noseworthy MD. Diffusion tensor imaging in evaluation of human skeletal muscle injury. *Journal of magnetic resonance imaging: JMRI*. 2006; 24(2):402–8. <https://doi.org/10.1002/jmri.20651> PMID: 16823776.
 17. Heemskerck AM, Drost MR, van Bochove GS, van Oosterhout MF, Nicolay K, Strijkers GJ. DTI-based assessment of ischemia-reperfusion in mouse skeletal muscle. *Magnetic resonance in medicine*. 2006; 56(2):272–81. <https://doi.org/10.1002/mrm.20953> PMID: 16826605.
 18. Takagi T, Nakamura M, Yamada M, Hikishima K, Momoshima S, Fujiyoshi K, et al. Visualization of peripheral nerve degeneration and regeneration: monitoring with diffusion tensor tractography. *NeuroImage*. 2009; 44(3):884–92. <https://doi.org/10.1016/j.neuroimage.2008.09.022> PMID: 18948210.
 19. Kershaw LE, Buckley DL. Precision in measurements of perfusion and microvascular permeability with T1-weighted dynamic contrast-enhanced MRI. *Magnetic resonance in medicine*. 2006; 56(5):986–92. <https://doi.org/10.1002/mrm.21040> PMID: 16986107.
 20. de Lussanet QG, van Golde JC, Beets-Tan RG, Post MJ, Huijberts MS, Schaper NC, et al. Dynamic contrast-enhanced MRI of muscle perfusion combined with MR angiography of collateral artery growth in a femoral artery ligation model. *NMR in biomedicine*. 2007; 20(8):717–25. <https://doi.org/10.1002/nbm.1133> PMID: 17295393.
 21. Faranesh AZ, Kraitchman DL, McVeigh ER. Measurement of kinetic parameters in skeletal muscle by magnetic resonance imaging with an intravascular agent. *Magnetic resonance in medicine*. 2006; 55(5):1114–23. <https://doi.org/10.1002/mrm.20884> PMID: 16598733; PubMed Central PMCID: PMC2041870.
 22. Larsson HB, Rosenbaum S, Fritz-Hansen T. Quantification of the effect of water exchange in dynamic contrast MRI perfusion measurements in the brain and heart. *Magnetic resonance in medicine*. 2001; 46(2):272–81. PMID: 11477630.
 23. Weinmann HJ, Laniado M, Mutzel W. Pharmacokinetics of GdDTPA/dimeglumine after intravenous injection into healthy volunteers. *Physiological chemistry and physics and medical NMR*. 1984; 16(2):167–72. PMID: 6505043.
 24. Wessig C, Koltzenburg M, Reiners K, Solymosi L, Bendszus M. Muscle magnetic resonance imaging of denervation and reinnervation: correlation with electrophysiology and histology. *Experimental neurology*. 2004; 185(2):254–61. PMID: 14736506.
 25. Hayashi Y, Ikata T, Takai H, Takata S, Ishikawa M, Sogabe T, et al. Effect of peripheral nerve injury on nuclear magnetic resonance relaxation times of rat skeletal muscle. *Investigative radiology*. 1997; 32(3):135–9. PMID: 9055125.
 26. Bendszus M, Koltzenburg M. Visualization of denervated muscle by gadolinium-enhanced MRI. *Neurology*. 2001; 57(9):1709–11. PMID: 11706118.
 27. Eisenberg HA, Hood DA. Blood flow, mitochondria, and performance in skeletal muscle after denervation and reinnervation. *Journal of applied physiology*. 1994; 76(2):859–66. <https://doi.org/10.1152/jappl.1994.76.2.859> PMID: 8175600.
 28. Furuno K, Goodman MN, Goldberg AL. Role of different proteolytic systems in the degradation of muscle proteins during denervation atrophy. *The Journal of biological chemistry*. 1990; 265(15):8550–7. PMID: 2187867.
 29. Kirsch GE, Anderson MF. Sodium channel kinetics in normal and denervated rabbit muscle membrane. *Muscle & nerve*. 1986; 9(8):738–47. <https://doi.org/10.1002/mus.880090810> PMID: 2431311.
 30. Shoji S. Effect of denervation on glucose uptake in rat soleus and extensor digitorum longus muscles. *Muscle & nerve*. 1986; 9(1):69–72. <https://doi.org/10.1002/mus.880090111> PMID: 3951482.
 31. Cangiano A, Lutzemberger L. Partial denervation in inactive muscle effects innervated and denervated fibres equally. *Nature*. 1980; 285(5762):233–5. PMID: 7374777.
 32. Clausen T. Regulation of active Na⁺-K⁺ transport in skeletal muscle. *Physiological reviews*. 1986; 66(3):542–80. <https://doi.org/10.1152/physrev.1986.66.3.542> PMID: 3016768.
 33. Kullmer K, Sievers KW, Reimers CD, Rompe JD, Muller-Felber W, Nagele M, et al. Changes of sonographic, magnetic resonance tomographic, electromyographic, and histopathologic findings within a 2-month period of examinations after experimental muscle denervation. *Archives of orthopaedic and trauma surgery*. 1998; 117(4–5):228–34. PMID: 9581249.
 34. Hindel S, Sohner A, Maass M, Sauerwein W, Mollmann D, Baba HA, et al. Validation of Blood Volume Fraction Quantification with 3D Gradient Echo Dynamic Contrast-Enhanced Magnetic Resonance

Imaging in Porcine Skeletal Muscle. PLoS one. 2017; 12(1):e0170841. <https://doi.org/10.1371/journal.pone.0170841> PMID: 28141810; PubMed Central PMCID: PMC5283669.

35. Hindel S, Sohner A, Maa M, Sauerwein W, Baba HA, Kramer M, et al. Validation of Interstitial Fractional Volume Quantification by Using Dynamic Contrast-Enhanced Magnetic Resonance Imaging in Porcine Skeletal Muscles. *Investigative radiology*. 2017; 52(1):66–73. <https://doi.org/10.1097/RLI.000000000000309> PMID: 27482651.